

IAC-22-A6.2, x67913

A MAP OF THE STATISTICAL COLLISION RISK IN LEO

Dr. Darren McKnight

LeoLabs, 4005 Bohannon Drive, Menlo, Park, CA 94025, USA, darren@leolabs.space

Ms. Erin Dale

LeoLabs, 4005 Bohannon Drive, Menlo, Park, CA 94025, USA, edale@leolabs.space

Dr. Rachit Bhatia

LeoLabs, 4005 Bohannon Drive, Menlo, Park, CA 94025, USA, rbhatia@leolabs.space

Mr. Chris Kunstadter

AXA XL, 200 Liberty Street, 25th Floor, New York, NY 10281, USA, chris.kunstadter@axaxl.com

Dr. Matthew Stevenson

LeoLabs, 4005 Bohannon Drive, Menlo, Park, CA 94025, USA, mstevenson@leolabs.space

Mr. Mohin Patel

LeoLabs, 4005 Bohannon Drive, Menlo, Park, CA 94025, USA, mpatel@leolabs.space

This paper summarizes the full suite of statistical collision risk products provided by LeoLabs that characterize the probability, consequence, and risk of debris-generating and mission-terminating collisions by object type and altitude. The population in low Earth orbit (LEO) comprises operational payloads, non-operational payloads, abandoned rocket bodies, large debris (> 10 cm, fragments and mission-related), and small debris (1 to 10 cm, lethal nontrackable, LNT). Considering these population categories, LeoLabs monitors and characterizes both the debris-generating potential in LEO and the mission-terminating collision risk. The global network of S-band radars built and operated by LeoLabs is starting to catalog some of the many thousands of sub-10 cm debris in LEO, “previously” LNT. These are not likely to create catastrophic debris-generating events but are likely to terminate the mission of an active payload upon impact. Statistical collision risk can be determined by aggregating single event conjunction data messages (CDMs) PCs and considering the masses of the objects involved. This information is compiled in the Conjunction Mapping Tool that maps the hot spots (i.e., local maxima of mass density, spatial density, PC, and risk) in LEO. This tool provides a means to compare and contrast the relative importance of space traffic management (STM, prevent mission-terminating collisions to operational payloads) and space debris management (SDM, includes debris mitigation and remediation). The regularly updated assessments from the Conjunction Mapping Tool provide insights into several recent relevant topics: (1) the risk posed by the breakup of Cosmos 1408, (2) identifying massive derelict objects for removal/remediation, (3) examining the consistency between traditional statistical collision risk with aggregate CDM risk, and (4) potential effects from the cataloguing of sub-10 cm debris.

I. INTRODUCTION

The space object population in Low Earth orbit (LEO) has increased significantly in the last few years with the number of trackable objects (by the 18th Space Defense Squadron and LeoLabs) numbering over 20,000 in the Summer of 2022. Over 5,500 of these being operational satellites.

Many tens of thousands more satellites are planned to deploy in the next five years. This frantic growth of agile and capable smallsats is layered on top of thousands of massive derelicts largely lingering from Cold War programs in clusters and presents a uniquely consequential debris-generating potential. A third, even more insidious component of debris growth in LEO

contributes significantly to the collision risk in LEO; on-orbit anti-satellite testing (ASAT) from two major events have spread debris throughout all of LEO.

This paper provides a detailed and fact-based mapping of how the three major LEO components – constellations of operational satellites, clusters of massive derelicts, and clouds of debris – largely drive the collision risk now and in the future.

II. TECHNICAL APPROACH

LeoLabs has a global network of radars comprised of six S-band and two UHF radars as of Summer 2022 located on four continents that generates over 500,000 radar measurements and three million Conjunction Data

Messages (CDMs) a day; the most prolific space situational awareness capability in the world. [1] This radar infrastructure is coupled with a scalable, cloud-based computational engine serving over 60% of operational satellites in LEO with collision avoidance (CA) services plus a variety of civil and military agencies worldwide with regulatory, tracking & monitoring, and space situational awareness (SSA) support.

CDMs created by this global space surveillance network are compiled, organized, and visualized with the LeoLabs Conjunction Mapping Tool to provide insights into the distribution of likelihood of collision and debris-generating potential by altitude, object type, and specific object. The probability of collision (PC) for a single close approach in LEO is provided by the CDM.

In reality, the PC is either 0 or 1; the PC value merely represents our confidence as to which outcome is likely to occur. While in everyday situations, one might be comfortable for low consequence events with a 50/50 chance of the event occurring to proceed without taking action to minimize the risk, as the consequence of the event increases the threshold for action becomes more stringent (i.e., a person is less comfortable accepting a large likelihood for a consequential event).

This threshold is partially a function of risk acceptance (as just noted) but also a function of the fidelity of the PC determination process. For conjunctions of space objects, the threshold for concern is much lower than everyday events (i.e., closer to 1/1,000,000 to 1/10,000 being a concern). For this reason, we include all events within a threshold of 1/1,000,000 (1E-6) for PC to aggregate and analyze conjunction events. The typical PC threshold on the order of 1E-5 to 1E-4 triggers a collision avoidance maneuver. [2]

The PC generated by the CDM is dependent primarily on the miss distance, positional uncertainty of each of the conjuncting objects, and the physical size of each object (i.e., hard body radius, HBR). [3]

It should be noted whenever an operational satellite is included in the CDM, the results portrayed by the LeoLabs-issued CDM (or the 18th Space Defense Squadron (SDS)-derived CDM) overestimates the PC since the operator with a Global Positioning System (GPS), or equivalent, receiver will likely have a smaller positional uncertainty than available through a radar observation.

For example, a GPS-derived state vector can be as accurate as 5 to 10 m while the LeoLabs-derived positional uncertainty for intact derelict objects and non-maneuvering payloads is on the order of 10-20 m and slightly worse for maneuvering spacecraft and debris fragments.

III. PC AND RISK BY ALTITUDE

The LeoLabs' Conjunction Mapping Tool is used to depict the PC and risk across LEO from January to June 2022 in Figures 1-4.

Figure 1 depicts all conjunctions with a PC > 1E-6 by PC level and altitude. The blue features of the plots represent the events involving at least one operational payload and any other resident space object; these events can be mitigated through Space Traffic Management (STM). The orange features represent conjunctions involving two debris objects where debris is considered intact derelict objects (such as items released during normal operations, abandoned rocket bodies, and non-operational payloads) and fragments (from explosions and collisions). These conjunctions can only be managed through Space Debris Management (SDM) such as debris mitigation to prevent the continued littering of LEO with debris or debris remediation whereby debris, already abandoned, is retrieved. This plot shows that STM PC peaks around 550 km and the SDM PC peaks around 850 km. Nearly 43,000 conjunctions with PC values above 1E-6 occur monthly on average in LEO. The total number drops to 15,000 (or 2,500/month) for PC > 1E-5 and 1,200 (or 200/month) for PC > 1E-4.

Figure 2 portrays the top 40 conjunctions as a function of PC and altitude. Overall, there are roughly the same number of SDM events as STM events when filtering by PC alone. The highest PC event was between two derelict Russian payloads on 3 March 2022 with a ~3% PC while the next three highest PC conjunctions involved operational payloads; remember the previous note about the likely slight over-estimation of STM PC values.

Figure 3 depicts all of the conjunctions monitored as a function of risk (i.e., PC times mass involved). This change in factoring highlights the importance of SDM events as many of them involve a pair of massive derelict objects at higher altitudes in LEO. Further, Figure 4 shows the top 40 conjunctions by risk (i.e., probability times consequence) and this filtering now the majority of events are SDM. Of the 40 riskiest events of the first half of 2022, 33 are SDM-related events and only seven STM-managed conjunctions. This highlights the importance of SDM which can be obscured if only the PC values are examined. This is especially true due to the trend toward smaller operational spacecraft and the fact that the actual final PC, as determined by the operator, is slightly smaller than assessed by LeoLabs. Notably, the highest PC conjunction of the year, noted previously between two derelict Russian payloads, is also the highest risk conjunction thus far in 2022.

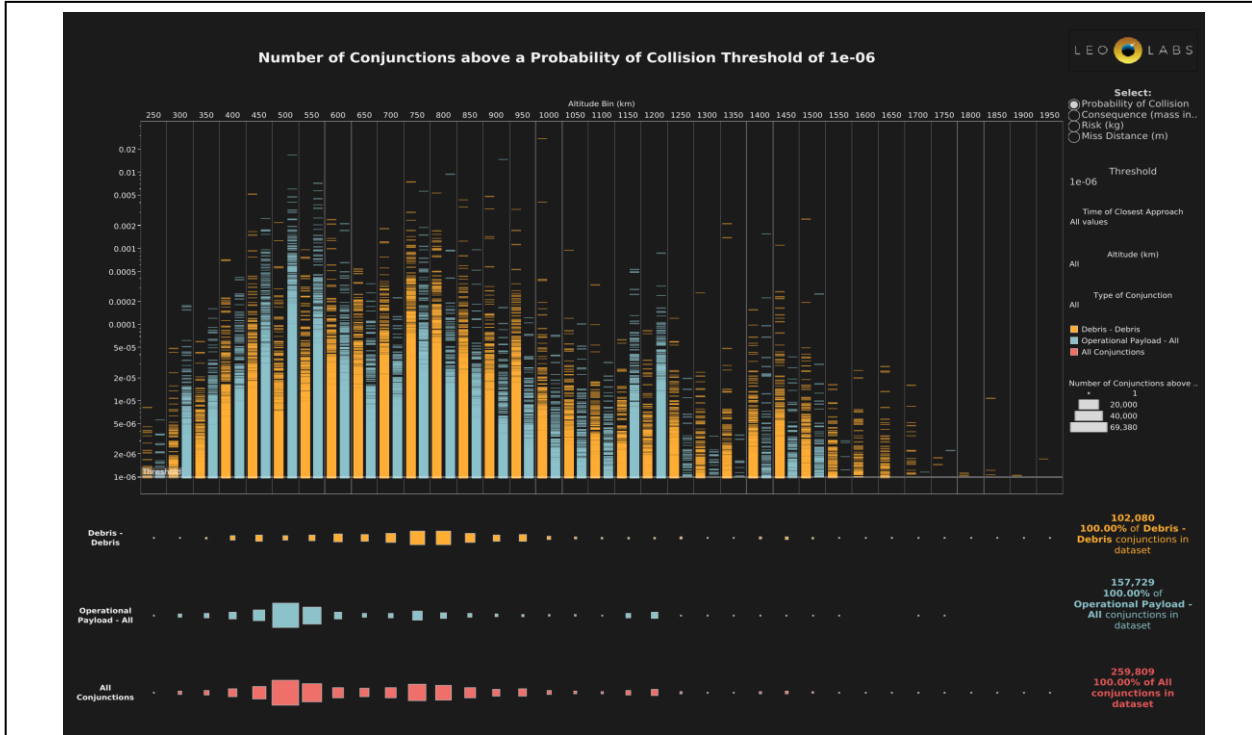


Fig. 1. The nearly 260,000 conjunctions captured by LeoLabs in the first half of 2022 (i.e., as of 30 June 2022) highlight the growing STM areas of interest between 500 to 600 km and lingering SDM concerns in spots from 700 to 850 km. Secondary peaks for STM and SDM are at ~1,200 km and ~1,400 km, respectively.

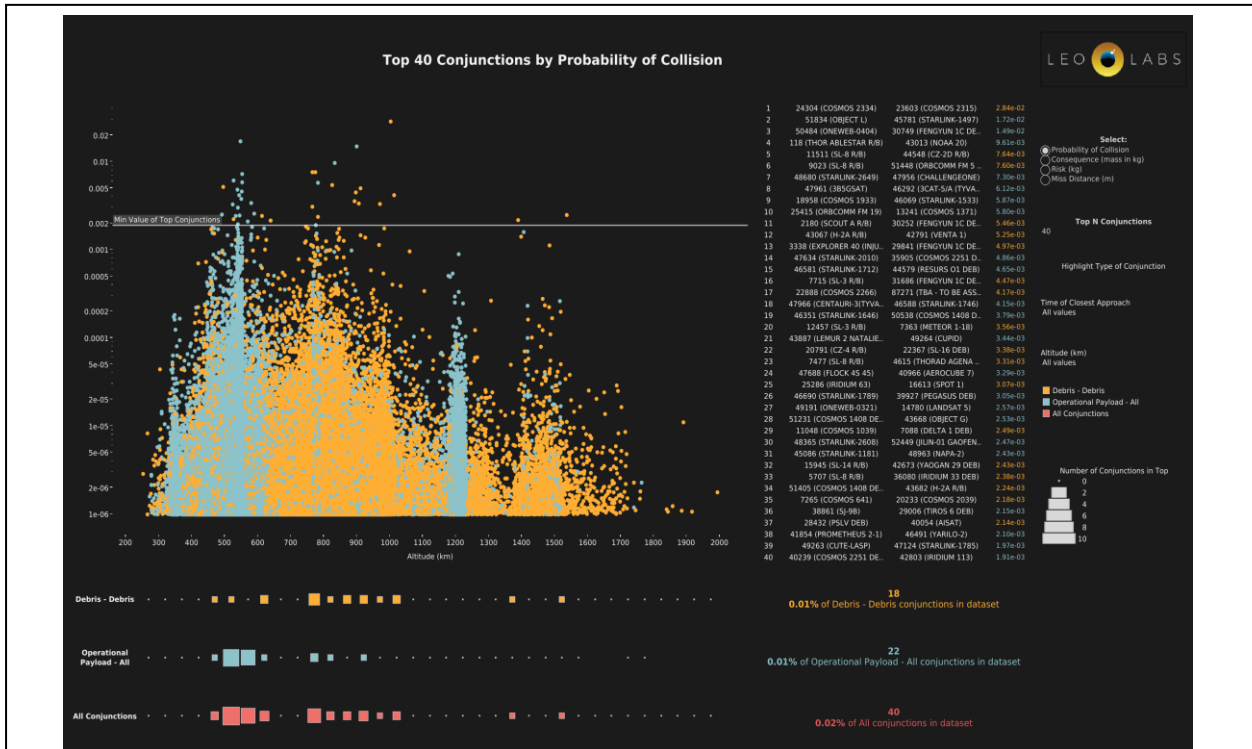


Fig. 2. The PC for the top 40 events plotted by altitude shows an apparent balance between SDM and STM events (i.e., roughly equal numbers of events out of the top 40 highest PC conjunctions).

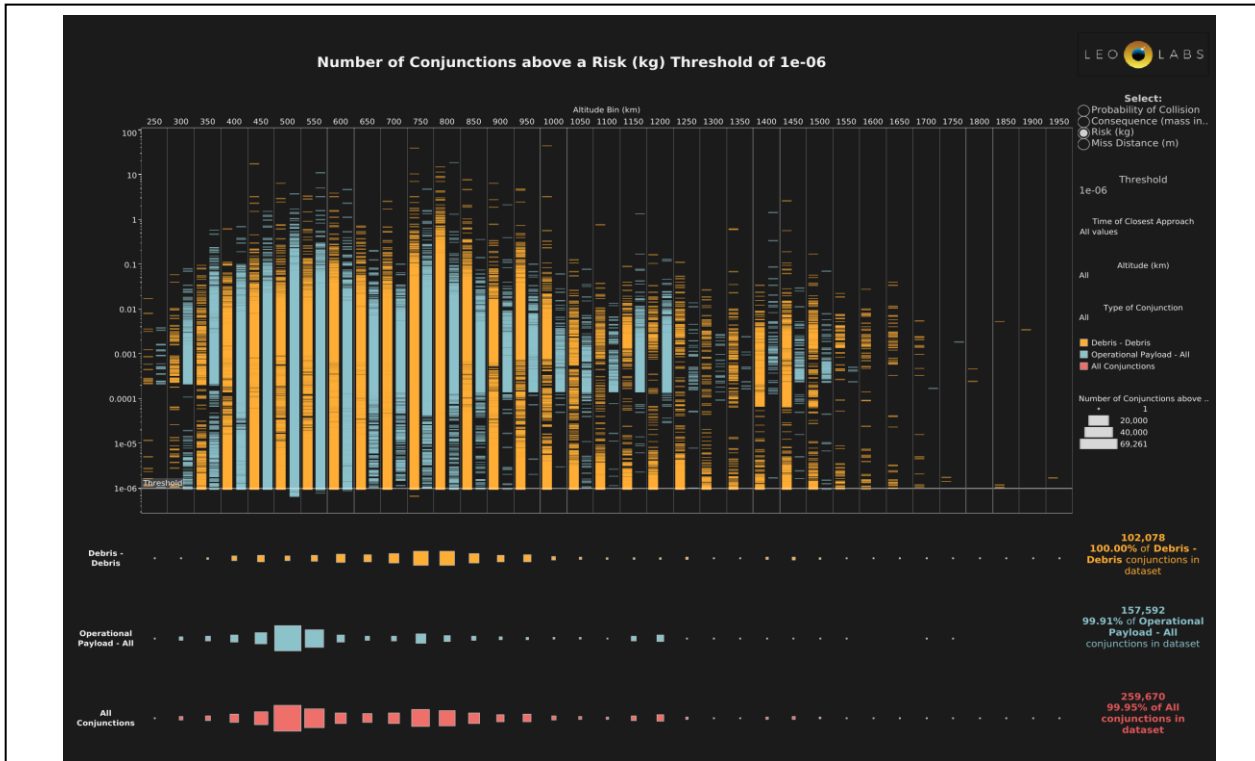


Fig. 3. Plotting conjunctions by risk changes the mapping in LEO with a swing toward more criticality in the SDM events (i.e., conjunctions often involving two massive derelicts).

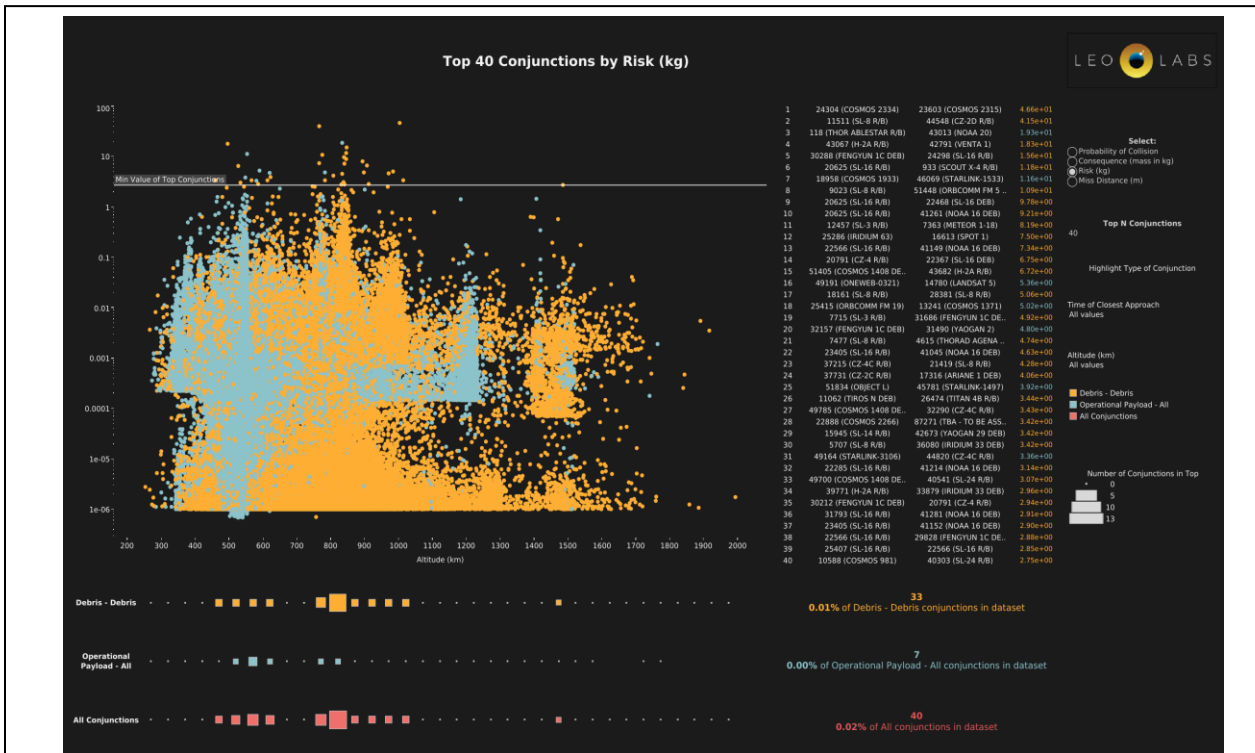


Fig. 4. The top 40 events by risk in the first half of 2022 accentuates the concern with massive derelicts in LEO with nearly five times as many of these conjunctions being SDM events rather than STM-related.

IV. PC AND RISK BY OBJECT FAMILIES

The mapping of conjunctions by altitude provides the first level assessment of the hazardous locations in LEO with regard to debris collisions. The next level of assessment is to consider what objects are creating this hazard.

Figures 5 & 6 depict the PC and risk by object families in LEO excluding operational payloads. Operational payloads (i.e., the blue STM events) are excluded since the PC is overstated by radar only measurements for most operational payloads that have onboard Global Positioning System (GPS), or equivalent and their collision risk is mitigatable to a large extent through collision avoidance maneuvers.

Figure 5 highlights the PC contributed by ASAT events such as Feng-yun 1C and Cosmos 1408 and also accidental debris-generating events such as Iridium-33, Cosmos 2251, NOAA 16, Delta 1 R/B, Resurs 01, Iridium 33, DMSP 5D-F13, CZ-4 R/B, NOAA-17, and SL-16 R/B.

Interestingly, the aggregate PC from Cosmos 1408 debris (declined from ~1,300 objects in January to ~800 fragments by the end of June) is still very close to the Feng-yun 1C ASAT debris cloud that contains nearly 2,500 fragments. However, there has been a significant dropoff in C1408-related conjunctions in May and June compared to the first four months of 2022.

At the same time, the maximum altitude conjunction event related to C1408 debris has also been dropped over time; it was over 1,400 km for the first four months of 2022, however, in June the highest registered high-PC conjunction was about ~1,000 km.

This reduction in apogee is likely to be seen as drag acts at an object's perigee. The lower altitude of the C1408 event and the rising solar activity helps in this process.

Further differentiating the two ASAT debris clouds, the Cosmos 1408 conjunctions have occurred predominantly (over 70% of the events) with operational payloads while less than a quarter of the Feng-yun 1C events involved an operational payload. The net result is the Cosmos 1408 debris has challenged triple the number of operational satellites than the Feng-yun 1C debris over the first six months of 2022.

Switching to a "risk filter" in Figure 6, amplifies the debris-generating potential concern for massive derelicts, especially high-altitude Soviet-era rocket bodies (e.g., SL-16 and SL-8). However, there are notable contributions by Chinese (CZ-2D and CZ-4C), American (Thor Able Star), and Japanese (H-2A) rocket bodies. Again, it is important to remind the reader while there are ~2,500 debris fragments from Feng-yun 1C still on orbit, there are only ~20 SL-16 R/Bs and ~290 SL-8 R/Bs.

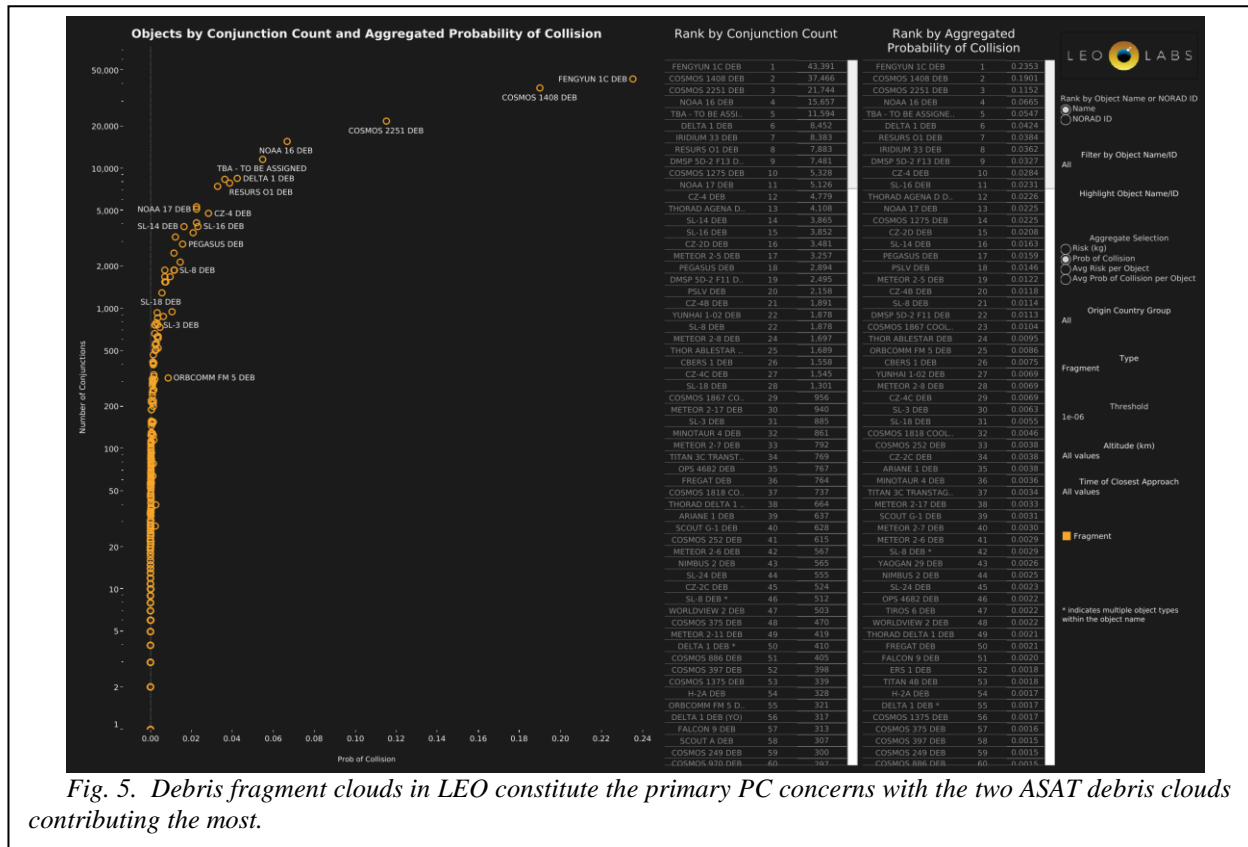


Fig. 5. Debris fragment clouds in LEO constitute the primary PC concerns with the two ASAT debris clouds contributing the most.

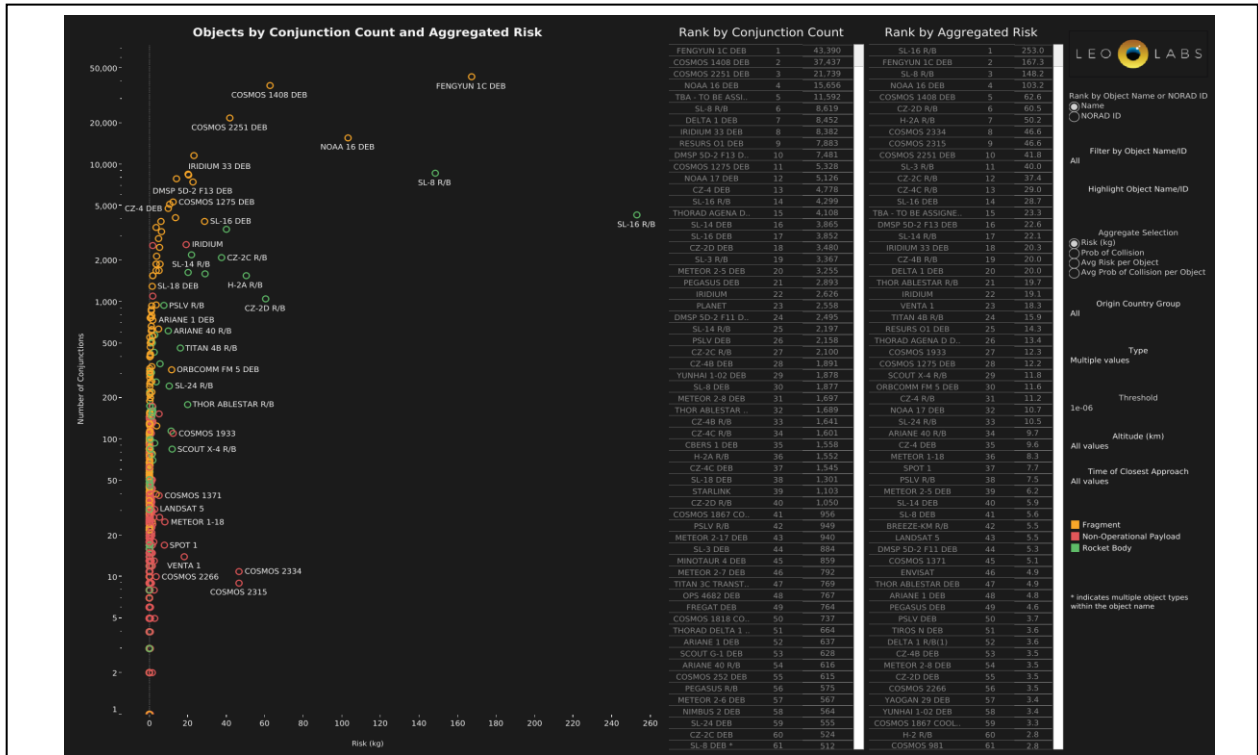


Fig. 6. Categorizing the aggregate risk for families of objects moves the massive derelicts such as SL-16 and SL-8 rocket bodies to the top of the list of concerns.

V. TOP FIFTY HIGH-RISK OBJECTS

In 2019, the top 50 statistically-most-concerning objects in LEO were identified primarily to suggest prime candidates for active debris removal (ADR). [4] Figure 7 shows the general decision filters for that paper and highlights the complexity of this type of assessment.

As has been emphasized thus far in the paper, risk (probability of an event times the consequence of that event) is the primary metric for this process. First, the PC can be determined both empirically and statistically.

The aggregating of the risk from the corpus of conjunctions monitored and reported by LeoLabs provides the foundation for the empirical data to support a new top 50 list.

However, the analytical likelihood of an event can also be determined by looking at the statistical probability of collision for any given object with the resident space object population with which it shares its orbit.

The consequence of any event, beyond the total amount of debris created, is amplified since it poses an immediate risk to operational satellites and/or by the debris being released at an altitude resulting in the debris remaining in orbit for many decades, or centuries.

Figure 8 shows the objects by satellite number (i.e., NORAD ID) that pose the greatest collision risk (i.e., probability times the amount of debris generated) as individual contributors. In essence, this is the graphical depiction of the top 50 (or more) objects in LEO.

The objects from Figure 8 are tallied in Table 1 with each satellite number, name, aggregate CDM risk, mass, and perigee/apogee. To refine the top 50 list, objects are

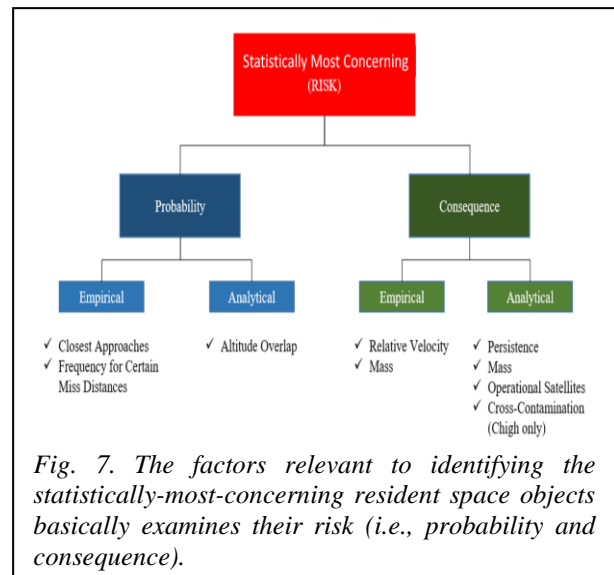


Fig. 7. The factors relevant to identifying the statistically-most-concerning resident space objects basically examines their risk (i.e., probability and consequence).

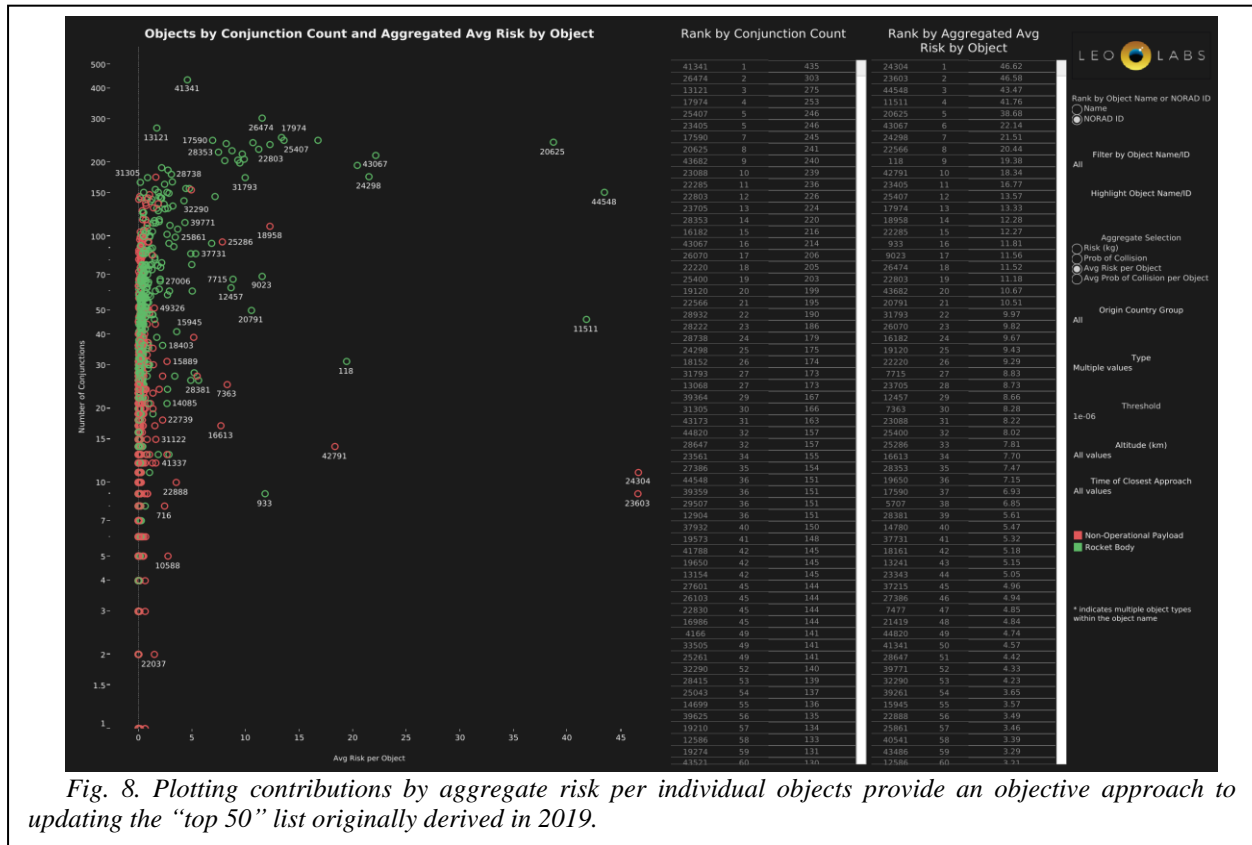


Fig. 8. Plotting contributions by aggregate risk per individual objects provide an objective approach to updating the “top 50” list originally derived in 2019.

removed if its average altitude is below 525 km or its mass is below 525 kg.

These filters were put on the selection process as smaller, shorter-lived objects will be less viable candidates for the expensive ADR process. Six objects were “removed” due to these restrictions but were left in the table and greyed out and lined through. Two objects were rejected due to low mass (Scout X-4 R/B and Venta 1) and four due to low altitude (H-2A, two CZ-4C, and Titan 4B R/Bs).

Table 1, as the new top 50 list, has the same caveat as the original list: as objects are removed, some other objects on the list may drop in importance.

The list contains 40 R/Bs and only 10 non-operational payloads. The original top 50 list had 39 R/Bs; just one short of the current list. By country, there are 36 with Soviet/Russian origin, five from China, five from the US, three from Japan, and one from Europe/ESA. The major change in this distribution from the original top 50 is the US having five members (up from zero) and China’s contribution rising from one to five.

The Soviet/Russian and European/ESA contributions decreased. Unlike the original top 50 list, the 20 SL-16s were not the first 20 objects, however, they are still prominent in the new top 50 list: all 18 of the SL-16s around ~840 km (and the one SL-16 at a

lower altitude) were included and accounted for five of the top ten and 19 of the top 35 objects.

Interestingly, the only repeat objects from the 2019 Top 50 list and the new one generated were these 19 SL-16 R/Bs and Envisat even though the general makeup of the top 50 (i.e., being mostly rocket bodies) changed very little.

The objects that were in the top five, moved ahead of the SL-16 R/Bs due a few very high PC conjunctions. An additional filter of a minimum number of conjunctions of 10 over this six-month study period had been considered. If implemented, the top two objects on the new list (i.e., Cosmos 2334 and Cosmos 2315) would have been eliminated (along with the Scout X-4 R/B which was already removed for having a mass less than 525 kg). These two payloads were involved in the highest risk conjunction for this study and this single event almost singlehandedly moved them to the top of the list.

This is a great example of the dependence between objects; if one of these two objects were removed from orbit, the other one would likely drop out of the top 50 list.

The primary change in this new top 50 list is the altitude distribution: the original top 50 list had 49/50 above 750 km but the new list has nine objects below 750 km average altitude.

Tab.1. The top 50 statistically-most-concerning objects are shown below with the greyed-out entries being removed either due to (1) mass being below 525 kg or (2) orbit being below 525 km to determine aggregate risk.

| # | SATNO (Object Name) | Aggregate Risk, kg | Mass, kg | Perigee, km | Apogee, km |
|----|---------------------------------|--------------------|-----------------|----------------|-----------------|
| 1 | 24304 (COSMOS 2334) | 46.62 | 820 | 964 | 1009 |
| 2 | 23603 (COSMOS 2315) | 46.58 | 820 | 967 | 1011 |
| 3 | 44548 (CZ-2D R/B) | 43.47 | 4000 | 756 | 765 |
| 4 | 11511 (SL-8 R/B) | 41.76 | 1434 | 756 | 780 |
| 5 | 20625 (SL-16 R/B) | 38.68 | 9000 | 833 | 854 |
| | 43067 (H-2A R/B) | 22.14 | 3000 | 457 | 615 |
| 6 | 24298 (SL-16 R/B) | 21.51 | 9000 | 841 | 862 |
| 7 | 22566 (SL-16 R/B) | 20.44 | 9000 | 833 | 851 |
| 8 | 118 (THOR ABLESTAR R/B) | 19.38 | 590 | 823 | 952 |
| | 42791 (VENTA 1) | 18.34 | 491 | 471 | 482 |
| 9 | 23405 (SL-16 R/B) | 16.77 | 9000 | 840 | 843 |
| 10 | 25407 (SL-16 R/B) | 13.57 | 9000 | 832 | 846 |
| 11 | 17974 (SL-16 R/B) | 13.33 | 9000 | 825 | 844 |
| 12 | 18958 (COSMOS 1933) | 12.28 | 1750 | 543 | 562 |
| 13 | 22285 (SL-16 R/B) | 12.27 | 9000 | 837 | 847 |
| | 933 (SCOUT X-4 R/B) | 11.81 | 37 | 523 | 2178 |
| 14 | 9023 (SL-8 R/B) | 11.56 | 1434 | 747 | 771 |
| 15 | 26474 (TITAN 4B R/B) | 11.52 | 4500 | 541 | 613 |
| 16 | 22803 (SL-16 R/B) | 11.18 | 9000 | 824 | 848 |
| 17 | 43682 (H-2A R/B) | 10.67 | 3000 | 516 | 590 |
| 18 | 20791 (CZ-4 R/B) | 10.51 | 2000 | 880 | 958 |
| 19 | 31793 (SL-16 R/B) | 9.97 | 9000 | 842 | 846 |
| 20 | 26070 (SL-16 R/B) | 9.82 | 9000 | 830 | 851 |
| 21 | 16182 (SL-16 R/B) | 9.67 | 9000 | 832 | 844 |
| 22 | 19120 (SL-16 R/B) | 9.43 | 9000 | 811 | 845 |
| 23 | 22220 (SL-16 R/B) | 9.29 | 9000 | 829 | 846 |
| 24 | 7715 (SL-3 R/B) | 8.83 | 1100 | 832 | 909 |
| 25 | 23705 (SL-16 R/B) | 8.73 | 9000 | 834 | 850 |
| 26 | 12457 (SL-3 R/B) | 8.66 | 1100 | 823 | 914 |
| 27 | 7363 (METEOR 1-18) | 8.28 | 1200 | 881 | 907 |
| 28 | 23088 (SL-16 R/B) | 8.22 | 9000 | 840 | 847 |
| 29 | 25400 (SL-16 R/B) | 8.02 | 9000 | 799 | 815 |
| 30 | 25286 (IRIDIUM 63) | 7.81 | 689 | 774 | 777 |
| 31 | 16613 (SPOT 1) | 7.70 | 1830 | 575 | 775 |
| 32 | 28353 (SL-16 R/B) | 7.47 | 9000 | 840 | 849 |
| 33 | 19650 (SL-16 R/B) | 7.15 | 9000 | 828 | 851 |
| 34 | 17590 (SL-16 R/B) | 6.93 | 9000 | 834 | 839 |
| 35 | 5707 (SL-8 R/B) | 6.85 | 1434 | 744 | 780 |
| 36 | 28381 (SL-8 R/B) | 5.61 | 1434 | 947 | 993 |
| 37 | 14780 (LANDSAT 5) | 5.47 | 1938 | 527 | 650 |
| 38 | 37731 (CZ-2C R/B) | 5.32 | 4000 | 603 | 687 |
| 39 | 18161 (SL-8 R/B) | 5.18 | 1434 | 952 | 996 |
| 40 | 13241 (COSMOS 1371) | 5.15 | 820 | 777 | 795 |
| 41 | 23343 (SL-16 R/B) | 5.05 | 9000 | 634 | 644 |
| 42 | 37215 (CZ-4C R/B) | 4.96 | 2000 | 675 | 800 |
| 43 | 27386 (ENVISAT) | 4.94 | 8211 | 764 | 766 |
| 44 | 7477 (SL-8 R/B) | 4.85 | 1434 | 959 | 1011 |
| 45 | 21419 (SL-8 R/B) | 4.84 | 1434 | 750 | 807 |
| | 44820 (CZ-4C R/B) | 4.74 | 2000 | 413 | 577 |
| 46 | 41341 (H-2A R/B) | 4.57 | 3000 | 534 | 558 |
| | 28647 (TITAN 4B R/B) | 4.42 | 4500 | 459 | 627 |
| 47 | 39771 (H-2A R/B) | 4.33 | 3000 | 571 | 596 |
| | 32290 (CZ-4C R/B) | 4.23 | 2000 | 396 | 469 |
| 48 | 39261 (CZ-4C R/B) | 3.65 | 2000 | 757 | 804 |
| 49 | 15945 (SL-14 R/B) | 3.57 | 1407 | 601 | 631 |
| 50 | 22888 (COSMOS 2266) | 3.49 | 820 | 947 | 1016 |

VI. COLLISION SCENARIOS AND MODEL

The mapping of conjunctions in LEO provides a hint at the most likely debris-generating collisions to occur. From the examination of over 1,000,000 conjunctions monitored and reported on by LeoLabs from 2020 through mid-2022, eight debris-generating collisions were derived as the most likely type of events to occur in the next 10 years. They are grouped into three categories in Table 2. An event similar to the nominal event (i.e., an SL-16 being struck by a large debris fragment) is the most likely event to occur and can be applied to immediate future growth scenarios with high confidence. Events similar to the next three collisions are considered moderately likely to occur in the near future. The last four events round out the types of high-consequence collision events possible to occur in the decade. Inclusion of these events, in addition to the first four events, should be considered a worst-case scenario with low confidence in all of these occurring. However, any one of these events is still on the list of most probable events to occur in LEO.

As LeoLabs continues to compile conjunctions, this suite of collision events will be refined. It should be noted we are not predicting any of these specific events will occur but rather these events are representative of debris-generating events that are most likely to occur. For example, there have been a steady number of explosions of abandoned rocket bodies during the space age; while we have not specifically “predicted” any specific explosion events there are eight rocket bodies included in the 16 objects for the eight scenarios from Table 2.

The number of catalogued objects generated by each

event used a simplified model tied to empirical observations from the breakups of Cosmos 2251, Feng-yun 1C, and Iridium-33 coupled with physics-based energy partitioning basics for explosions and collisions. The number of catalogued objects created are determined by the types of objects involved in the collision and the total mass of the two objects. Two payloads colliding assume the maximum energy absorption and yields two times the total mass involved in the event. (It should be noted this is conservative as the Feng-yun 1C event produced nearly four times the number of catalogued fragments as the mass of the target satellite in kilograms.)

The next most productive is a rocket body colliding with a payload; the debris generated is 1.5 times the mass involved. When two rocket bodies collide, the debris generation ratio is simply one (i.e., the number of catalogued fragments produced when two rocket bodies collide is approximated by the number of kgs of mass involved). Lastly, a trackable debris fragment striking an intact rocket body or payload is likely to produce about 0.25 times the mass of the derelict object.

As a side note, in previous analyses, the authors discussed the interesting nature of the debris cloud produced from the Cosmos 1408 ASAT test. [5] Due the hypothesized non-hypervelocity impact of the event (i.e., impact velocity less than 6 km/s) the anticipated number of catalogued objects relative to the mass of the target was predicted to be lower than for the other collision events analysed. Indeed, the fragment to mass ratio for Cosmos 1408 was only one while, as stated earlier, the Feng-yun 1C ASAT event had a ratio of four trackable fragments per kilogram of mass of the target.

Tab. 2. The eight breakup scenarios used to project potential future debris growth were derived from a large collection of conjunctions that LeoLabs has collected and analysed over the least two years.

| Altitude | Mass Involved, kg / Catalogued Debris | Object 1 | Object 2 |
|-------------------|--|---------------|-----------------|
| NOMINAL | | | |
| 836 km | 9,000 / 2,250 | SL-16 R/B | Feng-yun 1C DEB |
| MODERATE | | | |
| 782 km | 2,868 / 2,868 | SL-8 R/B | SL-8 R/B |
| 1,006 km | 2,250 / 3,375 | Cosmos 1709 | SL-8 R/B |
| 577 km | 1,100 / 275 | SL-3 R/B | Feng-yun 1C DEB |
| WORST CASE | | | |
| 838 km | 3,450 / 6,900 | Cosmos 1844 | DMSP 5B F5 |
| 1,510 km | 2,910 / 4,365 | Cosmos 1410 | SL-14 R/B |
| 948 km | 3,320 / 830 | CZ-2C R/B DEB | Cosmos 249 |
| 627 km | 5,410 / 5,410 | SL-14 R/B | CZ-2D R/B |

VII. STATISTICAL RISK VS CDM PC

Previous analysis comparing statistical PC with aggregate CDM PC displayed a large deviation from the notionally optimum ratio of one (i.e., statistical PC being identical to aggregate CDM PC). [6] There are a wide number of reasons why this might be the case with the primary issue being time over which this analysis was conducted. It is likely six months is a much shorter timeframe than needed for these two terms to possibly converge.

Figure 9 shows the ratio of statistical PC to CDM aggregate PC for 47 of the top 50 objects just reviewed. Three objects were eliminated from the top 50 list because they had very few conjunction events which skewed their results significantly. The remaining 47 objects actually had a smaller spread than the previous similar analysis. The median value for the rocket body ratios of Stat/CDM was very nearly a “perfect” one, with a median of 1.1. This means the typical statistical PC was, on average, equal to the aggregate CDM PC. Nearly all of the SL-16 R/Bs exhibited ratios above one (i.e., statistical PC greater than the aggregate CDM PC) while SL-8 rocket bodies were generally “below the line” (i.e., aggregate CDM PC greater than statistical PC).

The payload median ratio was 0.20; this may have

been due to the smaller sample size (i.e., seven total payloads and 40 rocket bodies).

The lack of convergence of this data to the “ideal ratio” of one is not unexpected for such a short duration experiment and without a more detailed examination of the limitations of the two models used to determine these values.

For example, the CDM PC may be a poor surrogate for PC if the PC values produced were “diluted” (i.e., covariance is much larger than the miss distance). [3] Upon examination of a subset of CDMs of the two objects with the most extreme Stat/CDM ratios in Figure 9, we discovered about 85% of all CDMs with diluted PC involve an operational payload. The maneuver capability of these objects could result in inflated uncertainty estimates for these objects and thus diluted PC.

Further, it should be noted that non-operational payloads and rocket bodies considered in Figure 9 are at different altitudes and different orbital regimes. This means the average velocity is most likely not the same. However, for this analysis a constant relative velocity of 12 km/s was used for the statistical risk. The variation in the average relative velocity from the given constant is also expected to affect the statistical PC estimate and result in divergence from a Stat/CDM ratio of one. To solve this, a study of the variation in the average relative

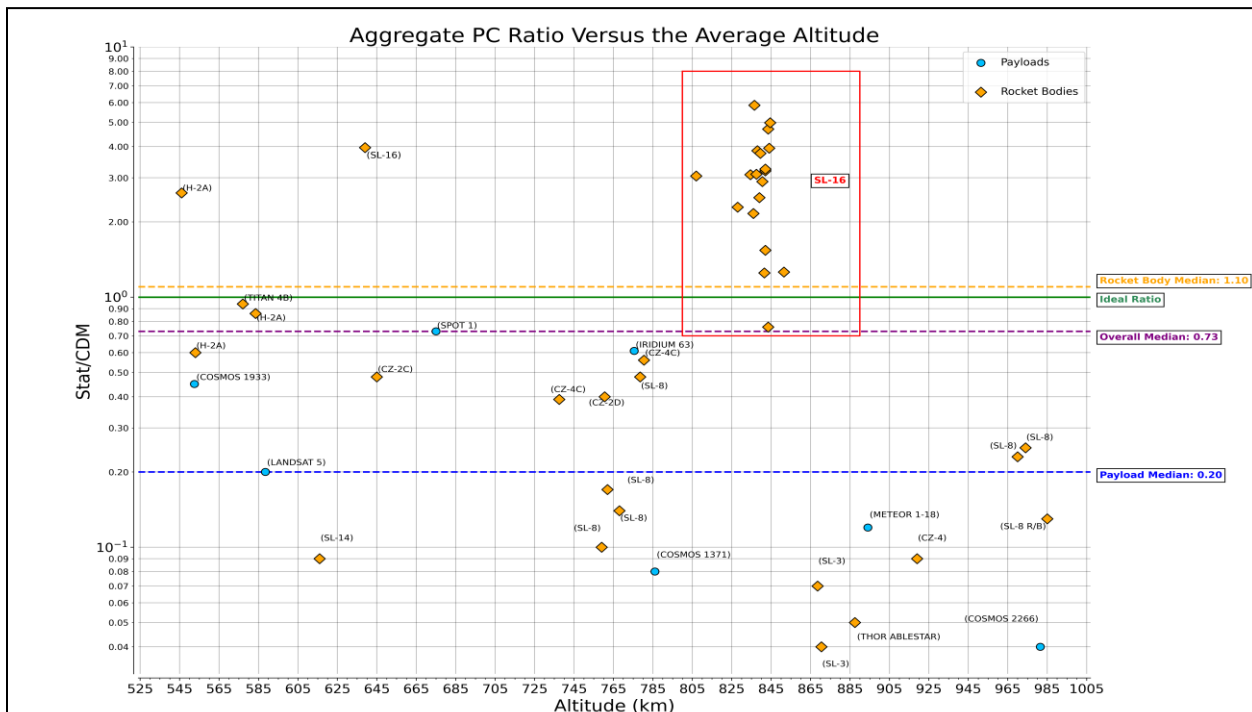


Fig. 9. The ratio of statistical PC to CDM aggregate PC mapped against altitude shows no real altitude dependence but does highlight that rocket bodies seem to have a better overall ratio (i.e., the median ratio is nearly one). The lack of convergence of this data to the “ideal ratio” of one is not unexpected for such a short duration experiment and without a more detailed examination of the limitations of the two models used to determine these values.

velocity for different altitudes and orbital regimes is underway and will be used to improve future modeling.

Lastly, it has also been noted that the statistical PC calculation is more sensitive to primary object HBR value than a CDM PC. This is because the statistical PC only considers the primary object HBR, the spatial density at the primary object' altitude bin, and the average relative velocity to determine the chance of at least one collision for the primary object, whereas the CDM PC uses the combined HBR of the primary and secondary object, the miss distance, and the uncertainty on both objects.

Since the CDM PC uses combined HBR as an input, it is relatively less sensitive to changes in the primary object HBR value. This explains the reason for the higher Stat/CDM ratio for SL-16 R/B (HBR value of 7.7 m) than that for SL-8 R/B (HBR value of 3.2 m).

LeoLabs will continue to tally and examine data relevant to this analysis theme as more conjunction events are monitored.

VIII. LEOLABS-ONLY (SUB-10 CM) CATALOG

The data presented thus far provides a detailed mapping of objects in LEO larger than 10 cm, nominally included in existing space object catalogs. However, there are likely many tens of thousands more fragments below 10 cm in LEO currently not in any catalog. As a result, there is no ability for operational satellites to avoid collisions with these objects likely to produce mission-terminating effects upon impact.

LeoLabs has initiated building a catalog of these objects (often referred to as lethal nontrackable debris, LNT). To be truly safe from the orbital debris collision hazard, these LNT must be included in actionable conjunction data messages (CDMs). It is anticipated that several thousand LNT will be added to the LeoLabs catalog over the next year.

Eventually this part of the catalog may potentially grow to include over 100,000 objects. CDMs have not yet been issued to space operators based on the preliminary objects added to this LeoLabs-only catalog as the process of discovering and cataloging these objects is in its infancy. It will likely take months before we report on the completeness or total number of objects in this growing catalog and their use in our mainstream collision avoidance services.

The ability to manage risk from these previously unaccounted for lethal objects is a significant contribution to space safety in LEO; in 2023, LeoLabs will be able to report on the total effect of the LeoLabs-only catalog.

IX. CLOSING COMMENTS

LEO is going through an explosive growth in satellite systems, but the backdrop of clusters of massive abandoned derelict objects and the clouds of debris from recent ASAT tests produce a headwind to the potential continued growth of LEO space commerce. Nearly 40% of the high PC conjunctions in the first half of 2022 involved a fragment from the two major ASAT tests conducted this century. Further, the region from 810 to 890 km has been highlighted as the worst "neighborhood" in LEO due to the negative contributions of the three major spacefaring countries over the last 45 years. While the major deployments of constellations appears to be above and below this troubled region, the effects of collisions in this region (and other altitudes) will have both immediate and long-term effects on altitudes most popular for constellation deployments (i.e., under 650 km).

The identification of the top 50 high-risk objects is eerily reminiscent of the top 50 objects identified in 2019. These highlight the need for a government-sponsored ADR programs to eliminate much of this pent-up debris-generating potential due to deployment and operations practices from the 1980s through 2010 largely in the 800 to 900 km altitude range.

The mapping of the probability of collision and debris-generating risk as a function of altitude provides a compelling message about space safety in LEO. Indeed, the growing number of operational satellites pose a growing operational concern, however, the remnants of decades of unregulated space operations (i.e., on-orbit anti-satellite testing and abandonment of large amounts of derelict space hardware in long-lived orbits have created significant safety and sustainability concerns for the operation of these new satellites.

REFERENCES

1. Reihs, B., Marshall, O., Williams, P., and Stevenson, M., "Increasing Capabilities in a Growing Radar Network," 73rd International Astronautical Congress, Paris, France, September 2022.
2. Starlink Satellites Still Dodging Orbital Debris From Russian Missile Test | PCMag
3. Alfano, Salvatore & Oltrogge, Daniel. (2018). Probability of Collision: Valuation, variability, visualization, and validity. *Acta Astronautica*. 148. 10.1016/j.actaastro.2018.04.023.
4. McKnight, et al, "Identifying the 50 Statistically-Most-Concerning Derelict Objects in LEO," 71st International Astronautical Congress (IAC) – The CyberSpace Edition, Dubai, UAE, October 2020.
5. New Analysis of Russian ASAT Provides Clues to Weapon's Trajectory, Says Risk From Debris Could Grow - Air Force Magazine

6. McKnight, D., Bhatia, R., Stevenson, M., and Dale, E., “Convergence of CDM Aggregate Risk and Statistical Collision Risk,” International Conference on Space Situational Awareness, Madrid, Spain, April 2022.